Do micro brown dwarf detections explain the galactic dark matter?

Theo M. Nieuwenhuizen[1], Rudolph E. Schild[2] & Carl H. Gibson[3]
Institute for Theoretical Physics, University of Amsterdam,
Science Park 904, P.O. Box 94485, 1090 GL Amsterdam, The Netherlands
[2]*Harvard-Smithsonian Center for Astrophysics, 60 Garden Street, Cambridge, MA02138, USA*
[3]*Mech. and Aerospace. Eng. & Scripps Inst. of Oceanography. Depts., UCSD, La Jolla, CA 92093, USA*
Correspondence to: Correspondence and requests for materials should be addressed to Th. M. N. (Email: t.m.nieuwenhuizen@uva.nl).
(Dated: April 17, 2011)

The baryonic dark matter dominating the structures of galaxies is widely considered as mysterious, but hints for it have been in fact detected in several astronomical observations at optical, infrared, and radio wavelengths. We call attention to the pattern of star formation in a galaxy merger, the observed rapid microlensing of a quasar by a galaxy, the detection of "cometary knots" in planetary nebulae, and the Lyman-alpha clouds as optical phenomena revealing the compact objects to be primordial gas planets in dense clumps that merge to form stars and globular star clusters. Radio observations of "extreme scattering events" and "parabolic arcs" are found to imply the same population of compact planet mass objects in interstellar space, and measurement of the cometary knots yield mass estimates of approximately earth mass as predicted. Estimates of their total number show that they comprise enough mass to constitute the missing baryonic matter. Mysterious radio events are explained by their pair merging in the Galaxy. Latent heat of evaporated hydrogen slowly released at the 14 K freezing transition at their surface explains the thermostat setting of the "dust" temperature of cold galaxy halos. The proportionality of the central black hole mass of a galaxy and its number of globular clusters is explained.

PACS numbers: 04.70.Bw,04.20.Cv, 04.20.Jb

Keywords: Galactic dark matter, MACHOs, galaxy merging, microlensing, cool dust temperature, cirrus clouds, Lyman-alpha forest, black hole

These authors contributed equally to the paper

I. INTRODUCTION

In 1931 Jan Oort realized that our Galaxy must contain invisible matter [1]. Fritz Zwicky soon concluded the same for clusters of galaxies, and called it dark matter (DM) [2]. The current paradigm of Cold Dark Matter (CDM, or ΛCDM including the cosmological constant) assumes it to arise from a heavy elementary particle with a small interaction cross-section. In the transition of the plasma of protons, electrons and He-ions to gas, the photons decouple and the baryons are said to condense on presumed pre-existing CDM condensations. However, despite many searches, this CDM particle has not been found [3] and this bottom-up scenario is stressed by numerous observations at its upper and lower size scales. On the largest scales, cosmic void structures are found on much larger size scales than predicted from simulations, whereas on the smallest scales, the many subhalos predicted to surround our Galaxy are not observed [4]. Moreover, the voids are emptier than simulated. And, the predicted "dark age" before the formation of stars and galaxies is coming more and more under stress with new observations of early structures arising basically every month [5, 6]. Neither does ΛCDM offer an explanation for the axis of evil [7], the dark flow [8], chain galaxies [9] or the bullet cluster [10], while correlations between galaxy parameters contradict the ΛCDM hierarchical clustering [11], as does the structure of the Local Group [12].

We shall follow an approach with two types of dark matter, "Oort" DM in galaxies, composed of baryons, and "Zwicky" DM in galaxy clusters, the true DM. Gravitational hydrodynamics or hydro-gravitational-dynamics (GHD or HGD) theory of structure formation assumes no new particle but only stresses the nonlinearity of hydrodynamics. It involves a top-down scenario starting with structure formation in the plasma at redshift z = 5100, well before the decoupling of matter and radiation at z = 1100 [13–15]. A viscous instability creates voids, which have expanded to ca 38 Mpc now, a fair estimate for the observed typical cosmic voids [16]. Just after the decoupling, all gas fragmented in Jeans clusters (JCs) of ca $6{\cdot}10^5$ solar masses, consisting of some $2 \cdot 10^{11}$ micro brown dwarfs (μBDs, muBDs) of earth mass, sometimes called MACHOs (Massive Astrophysical Compact Halo Objects). First stars occur by coagulation of μBDs, on gravitational free-fall time scales without a dark period. A fraction of Jeans clusters turned into old globular star clusters. Others got disrupted and became material for normal stars. But most of them still exist, though cold, and constitute the galactic dark matter. These dark JCs have an isothermal distribution, noticed in lensing galaxies [17, 18], which induces the flattening of rotation curves, while their baryonic nature allows to explain the Tully-Fisher and Faber-Jackson relations [15].

Nuclear synthesis attributes enough matter for the μBDs. About 4.5% of the critical density of the Universe is baryonic. At best 0.5 % is luminous, and a good 2% is observed in X-ray gas. So, the missing dark baryons may indeed be locked up in μBDs.

Questions about the nature of the baryonic dark matter (BDM) have largely been overshadowed in the past decade by even deeper questions about the non-baryonic dark matter. GHD just assumes that it is free streaming at the decoupling [15]. One of us in his modeling of the lensing properties of a galaxy cluster [19] confirmed that it should be related to cluster DM. Dark matter is described by an ideal gas of isothermal fermions, and galaxies and X-ray gas by standard isothermal models. This yields a DM mass of 1-2 eV, not the heavy mass of the hypothetical CDM particle. The best candidate is the neutrino with mass of 1.45 eV; a prediction that will be tested in the 2015 KATRIN tritium decay search. If also the right-handed (sterile) neutrinos were created in the early Universe, there should exist a 20% population of 1.45 eV neutrino hot dark matter, clumped at the scale of galaxy clusters and groups [19].

Returning to the problem of the more familiar galactic DM just consisting of baryons, it has probably been detected already in various observations but has not been considered in a single framework. The nature of the BDM seems obscure because nature places severe constraints, so it has thus far eluded detection. The BDM must be dominated by hydrogen in some form. Hydrogen can exist in its atomic form, as H_2 gas, or in ionized form, H^+. In gaseous form as H-clouds its strong signatures as radio (21 cm) and optical Lyman and Balmer alpha emission lines should have been observed in some kind of galaxy or other by now, creating a serious puzzle, that we solve here.

A second important impediment faced by the idea that the BDM is sequestered away in condensed objects is the formation question. It has long been concluded that hydrogen clouds cannot collapse to form planetary or solar mass objects because the hydrogen cannot cool quickly, and pressure forces will quickly restore the cloud. However these arguments all involve a simplifying assumption that the process can be linearized, whereas GHD starts from H condensed in μBDs. We now discuss that various types of observations support the GHD picture as the CDM theory flounders.

II. JEANS CLUSTERS VISIBLE IN GALAXY MERGING

The GHD formation theory predicts some $3 \cdot 10^{17}$ μBDs of earth mass per galaxy grouped in some 1.7 million Jeans clusters, each with mass $6 \cdot 10^5 M_\odot$, that constitute the galactic DM halos [13]. μBD merging has led to heavier objects like planets and stars.

As exposed in Fig. 1 of the Tadpole galaxies, galaxy merging turns the dark halo JCs into young (3-10 Myr) globular clusters (YGCs) along the merging path [15, 20]. Similar behaviors are observed in e. g. the Mice and Antennae galaxy mergers. The most luminous of the "knots" in Fig. 1 has an age of 4–5 Myr and estimated mass $6.6 \cdot 10^5 M_\odot$ [21], reminiscent of a JC. Observations generally reveal that the bright blue clusters are much younger (a few Myr) than the dynamical age of the tail (ca 150 Myr), providing strong evidence that star formation occurs in situ, long after the tail was formed [21]. GHD asserts that the cold μBDs along the merging path get warmed by tidal forces, which makes them expand and coalesce at suitable moments into young stars grouped in YGCs. The ΛCDM explanation as disrupted tidal tails [22] suffers from predicted but unobserved old stars.

Estimating the amount of galactic dark matter from fig. 1, the tail begins at 420,000 lyr from the center where it exhibits the sharp boundary of the dark matter halo. If there is spherical symmetry, the enclosed mass is $2.4 \cdot 10^{12} M_\odot$, a reasonable estimate. The opening width of 1500 lyr across remains fairly constant along the trail, as expected for an induced local heating effect. From an isothermal model the number of JCs in the wake can then be estimated as 5900, which within a factor of a few coincides with the number of bright spots in Fig. 1.

From these features one can already conclude that the galactic dark matter likely has the structure predicted by GHD.

III. QUASAR MICROLENSING BRIGHTNESS FLUCTUATIONS

Quasar micolensing has probably to date given the most compelling evidence that the BDM is contained in a network of planetary mass bodies with sufficient number to account for the entire baryonic dark matter. The first detection of this was made with brightness monitoring of the Q0957+561 A, B gravitationally lensed quasar, with two images A, B separated by 6 arcsec on the plane of the sky. 15 years of brightness monitoring revealed that a microlensing signal of amplitude 1% and time scale 1 day (observer's clock) was apparent in the data [23]. Because the signal was consistently observed for long periods of monitoring on a time scale of the monitoring frequency, 1 day, it was concluded that the microlensing originated in a population of compact objects having masses averaging $10^{-5.5} M_\odot$ and with other events up to Jupiter mass also seen.

Subsequent to this discovery, re-analysis of the quasar data [24] confirmed that the rapid fluctuations were not intrinsic to the quasar and therefore presumably microlensing. Furthermore the signal had an equal positive and negative network of peaks, as demonstrated from wavelet analysis [25]. This is understood to originate from a high optical depth and therefore is a signature that the μBD population observed in the lens galaxy must be the baryonic dark matter. This conclusion follows from a deep understanding of microlensing [26]. In general, the shear associated with gravitational lensing (macro, milli, micro, nano) causes a brightening event with a cusp-shaped profile. But in the presence of a macro-shear generated by the Q0957 lens galaxy G1, a micro-shear caused by a μBD in the lens galaxy would possibly further amplify the macro-shear or potentially de-magnify it on the micro-arcsec scale. Only in the special circumstance that the micro-shear originates in a population with unit optical depth to microlensing will the probability of micro-magnification and micro-demagnification be equal (p. 343 and Fig. 11.8 of Ref [26]) leaving a brightness profile with equal brightening and fading events on the time scale specific to the microlensing compact object, as simulated by [27]. Thus, the observed signature found to have approximately equal positive and negative events [25] uniquely indicates microlensing by a population at unit optical depth. Since the optical depth of

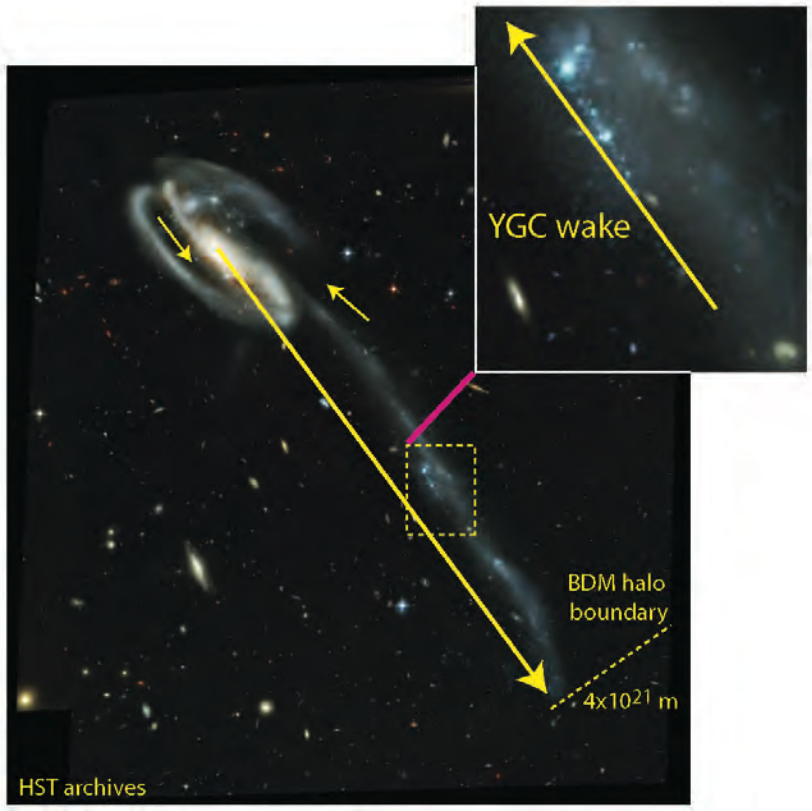

FIG. 1: As Tadpole galaxy fragments merge through the dark matter halo of the main galaxy VV29a, they exert tidal forces that trigger star formation of Jeans cluster cold micro brown dwarfs. The latter expand, coalesce and form new stars, turning the Jeans clusters into young globular clusters (YGCs). Forty-six YGCs appear as bright dots on a line pointing toward the point of merger of VV 29cdef fragments with VV29a in the insert [20]. The Tadpole tail VV29b was formed in place and not ejected by tidal forces. The diameter of the dark matter halo is eighty times the size of the central protogalaxy, and is formed by outward diffusion of Jeans clusters from the 10^{20} m protogalaxy, as their planets freeze.

image A is known to be 0.35 and of image B is 1.35, as determined by a model of the overall lensing that produces the double image, and since the lens galaxy G1 must plausibly be dominated by its baryonic dark matter, it may be concluded that the baryonic dark matter is detected as a population of μBD objects in the lens galaxy G1.

In an isothermal modeling, the average number of JCs along the quasar sightline A is 0.002 and for B 0.01. These numbers are close enough to unity to expect that along each sight line there lies exactly one JC. The estimated number of μBDs along the total light path then comes out as 18,000, confirming the observed multiple lensing events. The typical induced optical depth is 58, but the observed lower values occur if the light path traverses near the border of the JCs.

We are left with the extrapolation from theory and observation that the entire baryonic dark matter occurs in the form of a population of μBDs seen in microlensing of quasars by the grainy distribution of matter in the lens galaxy. The same population has been confirmed in several other lens systems [28–30], with microlensing mass estimates in the range $10^{-5.5}$ to $10^{-3} M_{\odot}$, that is, from individual μBDs to merged ones.

IV. COMETARY KNOTS IN PLANETARY NEBULAE

The μBDs are directly seen in the Helix and other planetary nebulae, see Fig. 2. Their infrared emission allows 20,000–40,000 of them to be counted in Spitzer [31]. They are found distributed in a band or shell at a central distance comparable to the Solar Oort cloud, $7 \cdot 10^{15}$ m. Because they are objects resolved at optical and infrared wavelengths, their sizes and structures

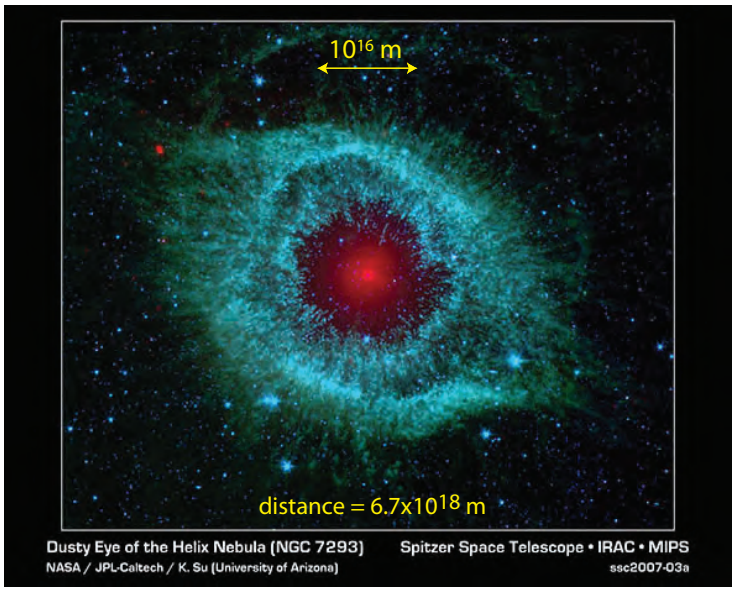

FIG. 2: Infrared observation by Spitzer of the Helix planetary nebula. The white dwarf in the center is surrounded by an Oort cavity around which some 20,000–40,000 micro brown dwarfs are observed in a band perpendicular to the line-of-sight. They are visible due to heating by the plasma jet of the white dwarf.

may be estimated. Since they are radio CO emission sources, their masses may be estimated from their total CO emission and a normal CO/H emission ratio [32]. They have a cometary shape which allows their masses to also be estimated from an ablation theory applied to their outer atmospheres [33]. Both methods yield mass estimates between 10^{-6} and $10^{-5} M_{\odot}$. The current literature often explains them as Rayleigh-Taylor instabilities in the outflowing nebular gas. However, RT instabilities would not cause strong density contrasts in the ambient gas. Density contrasts of only 4-6 would be expected from the Rankine-Hugoniot supersonic jump condition, whereas density contrasts of 1000 are observed from direct mass estimates [33]. Attempts to measure their proper motions by comparing HST images at different epochs have been carefully done to define whether they have expanding or static distributions [34], but the results have been inconclusive. The gas outflow velocity of [35] does not refer to the proper motion measured expansion of the system of knots.

V. ON DIRECT MACHO SEARCHES

With gas clouds apparently absent, the community turned, in the 1990s, to searches for condensed hydrogen-dominated objects and initiated microlensing searches for them. The MACHO [36–38], EROS [39–41] and OGLE [42–44] programs all found microlensing events in front of the Large and Small Magellanic Clouds (MCs) and the galactic center. Early claims that the few detections implied a population of white dwarfs were not substantiated because the population of progenitor stars could not be identified. Most observed objects are white dwarfs, Jupiters or Neptunes, probably inside the MCs and galactic center.

From GHD one expects all galactic DM of earth mass μBDs. This case is just allowed by the MACHO collaboration [36], but ruled out by EROS-1 [40]. However, for observations against the Magellanic clouds, the estimate for the radius of the μBD of $2.6 \cdot 10^{11}$ cm coincides with its typical Einstein radius, leading to the microlensing unfriendly finite-source finite-lens situation [45, 46]. Obscuration by μBDs and refraction by their atmospheres may have hindered the observation of Macho events.

For the μBDs now predicted to be grouped in JCs, blind searching is not optimal. The JCs in front of the Magellanic clouds can be identied from WMAP, Herschel or Planck imaging data. See them also in the DIRBE-COBE image of fig 3. They should be a fertile ground for MACHO searches, but the observation cadence must be greatly increased because of the low mass of the μBDs. For a terrestrial mass MACHO passing in front of a small star the total event duration is approximately 3.5 hrs. For μBD microlenses clustered with properties measured for ordinary globular clusters, some 4,100 events should be visible per year by a dedicated spacecraft that continuously monitors the stars behind any of the 3400 JCs in front of the MCs. The number would increase if a clump of clusters as described below lies in front of the LMC. There should also be multiple events on the same star.

VI. HALO TEMPERATURES AND CIRRUS CLOUDS

If most of the baryonic dark matter is sequestered away from view in μBDs its thermal emission should still be seen as structured far-IR or sub-mm emission. The μBDs would have been warmer than ambient gas at time of μBD formation, and with their gravitationally heated cores they would be radiating heat away to the universe. Initially this would have cooled the objects significantly on time scales of 1 million years, since it has already been noticed that they are observable as T-dwarfs only in the youngest star forming regions [47]. Thereafter they would have continued to cool in the expanding and cooling universe, but with large cooling blanketing atmospheres they should then have cooled slowly.

Because hydrogen has a triple point at 13.8 K, higher than the 2.725 K cosmic microwave background, phase transitions with significant heats of condensation and fusion have the potential to act as a thermostat to set the temperature of the baryonic dark matter, thus explaining the cool galactic dust temperatures of < 20K [48] and 14–16K and 15–25K [49] as galaxy haloes. Indeed, cooling atomic hydrogen at low density and pressure passes slowly through its triple point, so the μBD population should have dominant thermal emission at or slightly above this temperature. The wavelength of peak emission would be 210 microns, or .21 mm. A detection of this thermal signature has also been made in a careful comparison of IRAF, DIRBE, BOOMERANG, and WMAP images for a Halo region of our Galaxy. These show [50] that the observed structure radiates at approximately 16K and has its peak radiation in the 220 micron DIRBE band. In fig. 3 we show one panel of fig. 2 of [50], which is now understood to be an image of the baryonic dark matter, seen in its emission peak wavelength. Although the far-IR emission of the Halo has been described as "cold dust cirrus" we find from direct imaging a clumped distribution, even with nested clumps, which suggests an interpretation of it as a clumpy distribution of JCs.

This view is supported by the amplitude of the signal. The standard Planck intensity at the DIRBE frequency of 1.25 THz caused by a thermal μBD atmosphere at 15 K is 54 GJy. With an μBD radius of $2.6 \cdot 10^9$ m and the typical distance to the next JC equal to $8.9 \cdot 10^{18}$ m, the Planck intensity is attenuated by the square of their ratio to become 0.9 kJy for the whole JC, about the highest observed value in [50]. Moreover, that nearest JC would have an angular diameter of 0.6°, slightly less than the largest structure of Fig. 3. Next, the intensity per solid angle can be estimated as 12 MJy/sr, mildly overestimating the maximal scale of 2 MJy/sr of several objects in Fig. 3. We can also estimate the number of structures in Fig. 3. From an isothermal model we predict about 67 structures larger than 0.25° in diameter, which is a fair estimate.

With reasonable estimates for their intensity, angular width and number, it is likely that the concentrations in Fig. 3 arise from the JCs that constitute the full Galactic dark matter. Non-baryonic dark matter is relevant only on galaxy cluster scales.

A further aspect is the size of the μBD atmospheres. For redshift $z > 4$ the ambient temperature is above the triple point and atmospheres are large. After that, liquid drops form in the outer atmospheres which rain onto the center. This will lead to a sizable shrinking of the atmospheres, and enhanced transmissivity for radiation, an effect similar to the reionization of the inter cluster gas. The latter may be caused by neutrino condensation on the cluster [19].

VII. RADIO EVENTS WITH FIXED SOURCES

Extreme Scattering Events were discovered as radio brightness anomalies in quasars. An event was characterized by 30% amplitude fluctuations with a cusp-profiled signature that is somewhat frequency dependent. This allowed them to be understood as a refraction event caused by a centrally condensed gaseous object passing in front of the quasar with a transverse velocity of a few hundred km s^{-1}, the radio analogue of the above quasar brightness fluctuations. A physical model was quickly developed, which included refraction by an ionized outer atmosphere acting as a negative lens that produces the observed pattern of brightness cusps [51]. The objects were described as self-gravitating clouds with approximately spherical symmetry. In the refraction model, an electron column density of $10^{20}\mathrm{m}^{-2}$ is determined. The atmospheres of the objects have a size of 1 AU ($1.5 \cdot 10^{13}$ cm), and must be gravitationally bound or else confined by an ambient pressure. We notice a similarity to the properties of the μBD discovered in quasar microlensing. The ESE clouds would be self-gravitating, have mass less than $10^{-3} M_\odot$, have a size of $10^{14.5}$ cm, are a Halo population, and have typical galactic speeds. Not surprisingly, it is independently estimated that the observed objects may relate to a good part of the galactic DM [51].

A probably related phenomenon is the crescent shaped events seen in the timing data in pulsars, since like the Extreme Scattering Events in quasar brightness curves, the pulsar anomalies are attributed to a refraction phenomenon due to condensed objects along the sight lines. It is inferred that the refraction effect produces multiple images of the pulsar radio signal, and interference of the images causes the observed phenomena. The scattering medium is estimated to have structure on 1 AU for a 10^3 interstellar density enhancement [52]. This corresponds to a radio scattering atmosphere of 10^{16} kg, as expected well below the GHD prediction of an earth mass for the entire object.

VIII. MYSTERIOUS RADIO EVENTS AS μBD MERGINGS

Recently, a mysterious class of "long duration radio transients" has been observed, lasting more than 30 minutes but less than several days, that have neither a counterpart in the near-infrared, visible or X-ray spectrum nor a quiescent radio state. The event rate is very large, $\sim 10^3 \mathrm{deg}^{-2}\mathrm{yr}^{-1}$ and they can be bright (> 1Jy). They were attributed to old galactic neutron stars [53], but this would lead to a prediction of more luminosity for distant galaxies than observed.

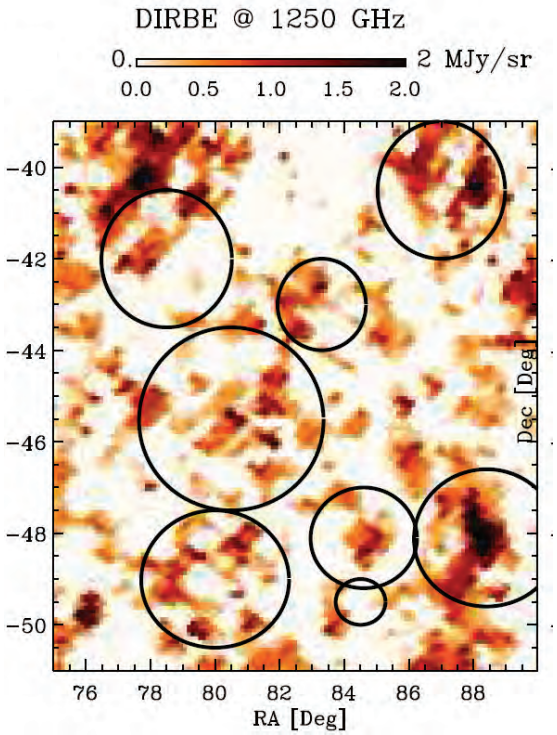

FIG. 3: The DIRBE map of a 15×12 degree region of the Halo, taken from Fig. 2 of [50], with black circles denoting regions of focus. Emission knots at the 240 micron peak of the thermal emission at the 15 K freezing-boiling point of hydrogen are here explained as a few hundred optically dark Jeans clusters at various distances aggregated in clumps.

Within GHD it is natural to connect these events to μBD mergings in the JCs that constitute the BDM halo of the Galaxy. Let us present a statistical estimate for the event frequency. For the typical duration we take $t_{ev} = 1$ day, so the effective μBD radius is estimated as $R_{bd} = v_{bd}\, t_{ev} = 2.6 \cdot 10^{11}$ cm. The typical JC has $(R_{jc}/R_{bd})^3$ cells of linear size R_{bd}. At a given moment in time the average number of μBD pairs that occupy the same cell in a given JC is 0.5. In the Galaxy the number of Jeans clusters is $1.7 \cdot 10^6$. The resulting rate of merging events is $7400/\mathrm{deg}^2\mathrm{yr}$, modestly overestimating the observed value.

The amount of gravitational energy available in the merging process is large, of order GM_{bd}^2/R_{bd}, which means some 10^5 J/kg. Assuming this to be emitted at distance of 3 kpc during the event time of 1 day in a frequency band of 10 GHz gives a bright radio event of 1 Jy; such events are observed, see table 2 of [53]. Ofek et al. also discuss scenarios for the emission in radio such as synchrotron radiation.

IX. DIRECT DETECTION IN NEARBY STAR FORMING CLOUDS

Recently a 2-3 Jupiter mass object has been discovered in the ρ Ophiuchus star forming region [47]. Estimated properties were a T spectral type, a surface temperature near 1400 degrees K, and an age of one million years. At its inferred distance of 100 pc it is presumed to be a member of the ρ Ophiuchus cloud region because of its heavy visual absorption. Since active star formation in the region is underway, it is inferred that the object has formed in the standard cloud collapse scenario, and represents an object near the bottom of the stellar mass function. It cools quickly (in about a million years), so that it may represent a population of planet-mass MACHO objects. With reasonable assumptions about their luminous lifetimes and number, they have been inferred to be a cosmologically significant population [47]. In GHD one sees the Jupiters as clumps of μBDs, that may go on growing to a star. Hence this observation hints at the population of μBDs.

This discovery is discussed [47] in the context of the many similar objects found in the most active star forming regions in Orion [54, 55]. All these authors recall that such objects would not form in the framework of the standard linearized theory of star formation, and appeal to fragmentation models [56] which, however, seem incompatible with the extreme binarity seen in the statistics of double stars and our solar system's Kuiper Belt Objects.

In Table 1 we show multiple estimates of the same physical parameter where they have been independently estimated in

different research programs related to the muBDs.

Estimator	microlensing	ESE	Cometary knots	T dwarfs
Log Mass ($M_\odot$)	–5.5	< -3	–5.3 (–5.2)	–2.6
Log radius (cm)	–	14.5	15.6	9.9
Log density (cm^{-3})	–	12	6,(5.9), (5.6)	24.2
Velocity (km s^{-1})	600	500	–	–
Cosmological Signf.	yes	yes	–	yes

Table 1. Measured and inferred properties of micro brown dwarfs from various observations. ESE = Extreme Scattering Events.

X. INFERRED SOURCE OF LYMAN-ALPHA CLOUDS

In quasar spectra a population of thousands of hydrogen-dominated clouds is seen causing weak absorption lines called the Lyman-alpha forest. Their properties have been reviewed [57]. Since they are detected as redshifts of the 1216 Å Ly-α line and are sometimes accompanied by higher level Lyman lines, their identification is secure. In a typical spectrum, one or two stronger and damped lines are also seen. In these cases there are weak metallic absorption lines at the same redshift. Because they are found along sight lines to cosmically distant quasars, much is known about their distribution from their redshifts. They are known to be relatively uniformly distributed in redshift, with, however, mild clumping at distance/size scales of 20 Mpc, showing the cosmic pattern of voids on scales of 30 - 130 Mpc. The depth of cloud absorption lines and their numbers increase with redshift z. Perhaps their most interesting property from a structural point of view is the velocity width parameter measured for each line. The average value is approximately 30 km/s, which suggests that as clouds they should dissipate on a time scales of several years. Their observed permanence was first presumed to imply that the clouds were confined by a hot inter-cluster medium, which was searched for but not found. This has left the subject with no explanation for their structure and common existence.

We propose that the clouds are in fact outer atmospheres of the μBD population in JCs detected in other observations as inferred above. JCs intersecting by the quasar sight line lie in a cylinder, so their mass can be estimated as $0.02\rho_c \cdot \pi R_{jc}^2 \cdot c/H_0$, where the factors describe the average cosmic baryon density not in X-ray gas, the JC surface area and the typical quasar distance, respectively. Though this corresponds to 0.0001 JCs only, a few thousand may actually occur because matter is clumped in filaments between voids, where the baryonic density may be 5-10 times the mean galactic mass density, i.e. about $10^7\rho_c$. In a JC located close to the quasar, about 900 μBDs will lie in front of it, which by their random motion at 30 km/s cause an absorption line of width 30 km/s. This number becomes lower for JCs closer to us, because the opening angle of the quasar covers less of their surface. At higher redshift the μBD atmosphere will be warmer and larger, which explains the increase of Ly_α absorption with z [57].

We attribute the broad absorption lines corresponding to b = 200 km s^{-1} to a set of JCs along the line of sight with this velocity dispersion typical for objects in galaxies, while the involved mass could then be large enough to expose the metal lines. With most JCs located in galaxies, the typical number of JCs per galaxy pierced by the light path of the quasar is 0.001, which explains that per few thousand narrow absorption lines there will typically be a few broad ones.

XI. IRON PLANET CORES

A perplexing problem is the origin of the magnetic iron cores of the Earth, Mercury and Neptune. It is well known that most of the metallic atoms in the universe are seen in meteoritic dust as oxides of iron, silicon etc. So it is difficult to imagine how the iron was reduced to metallic form underneath an ocean of water. However, primordially formed μBDs offer a direct scenario. From their periodic mergings to form larger planets and eventually stars, they have well-mixed and massive gas and liquid-solid hydrogen layers with wide temperature ranges that gravitationally sweep up and reprocess iron and nickel oxide supernova II star dust from the interstellar medium [58]. Metal oxide dust grains meteor into the hydrogen layers where reaction kinetics and hot mixing mergers reduce iron, nickel and other oxides to metals in solid and liquid forms that sink to form dense metal core layers under oxide layers (rocks, water) with cold outer hydrogen layers. Planets near the sun lose most of their hydrogen atmospheres in their pre-stellar accretion discs and by the solar wind.

Enormous numbers of hydrogen-1 helium-4 planets are produced by the cosmological big bang according to HGD cosmology. Approximately 10^{80} planets in 10^{68} Jeans mass clumps form the baryonic dark matter of the protogalaxies before the first star. All stars form by a sequence of binary mergers of the planets from earth-mass to solar-mass, a million-fold increase in mass. The first stars after the plasma to gas transition should occur in the gravitational free fall time of the Jeans mass clumps of planets; that is, in about 30,000 years. The first supernovae and the first chemicals should be scattered among the trillion planets of the clumps in the same time interval.

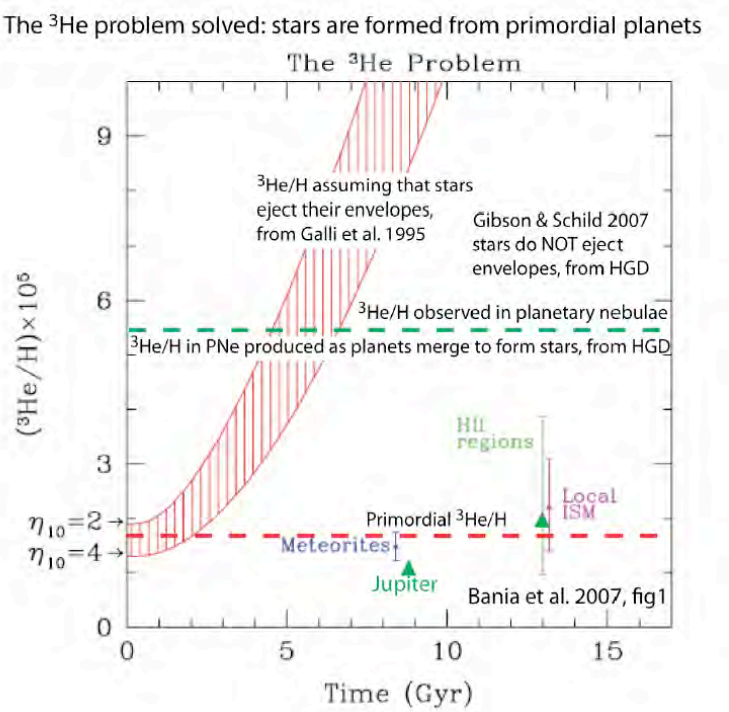

FIG. 4: Solution of the helium-3 problem [63] is provided by hydrogravitational dynamics HGD, where all stars are formed by primordial planet mergers, and do NOT eject stellar materials in massive shells as claimed by the standard models of star formation.

As the first chemicals seed the gas planets the oxides will be rapidly reduced, giving metal cores with molten rocky oceans. These cores are re-cyled periodically. As the planets merge, the metal cores become more massive, the lava oceans become deeper and the hydrogen-helium pressures become larger as the gas atmospheres also merge. Organic chemistry begins promptly in the planet atmosphere as the carbon dioxide becomes monoxide, hydrogen cyanic acid etc. in the hot, dense, moist atmospheres. Finally water oceans condense at 2 million years when the temperature of the universe cools to the critical temperature of 647 K. Only a few rare planets in close solar orbits like Mercury, Venus, Earth and Mars lose their hydrogen dominated atmospheres in favor of oxides.

Critical temperature water oceans in cometary communication provide a cosmic primordial soup for the evolution of life processes [59]. At 8 million years the temperature of the universe cools to 373 K, the freezing point of water, and the biological big bang does not cease but certainly could be expected to slow down.

XII. BLACK HOLES, YOUNG STARS AND GLOBULAR CLUSTERS

Our conclusion that the long sought baryonic dark matter has been observed already as micro brown dwarfs of planetary mass has implications for the formation process of planets and stars. The observation of young stars (age ∼1 Myr) in a disk near the black hole (BH) in the center of our Galaxy known as Sag A*, is difficult to explain and termed the "paradox of youth" [60]. A new scenario is offered by GHD: in a Jeans cluster passing close by the BH the μBDs were heated by the strong tidal forces, they expanded and coagulated in situ into new stars; this JC got disrupted and its stars ended in a plane.

Tidal forces by heavy central BHs may generally have a strong impact on nearby passing JCs. Let us suppose that JCs have an appreciable chance to be transformed into a globular star cluster (gc) when their gravitational energy $GM_{BH}M_{jc}/R$ exceeds a certain bound E_c, which happens when they pass within a distance $R_* \sim M_{BH}$. In an isothermal model their number $N(R_*)$ is proportional to R_*, explaining that $N_{gc} \sim N(R_*)$ is proportional to M_{BH}, in accordance with the observation $M_{BH} \sim N_{gc}^{1.11\pm0.04}$ [61].

XIII. HELIUM-3 IN PLANETARY NEBULAE

Nucleosynthesis following the cosmological big bang event permits formation of mostly hydrogen and helium-4, with only trace amounts of hydrogen-2, hydrogen-3 and helium-3. The primordial helium-3 to hydrogen-1 ratio is $1.4 \cdot 10^{-5}$ [62]. HGD cosmology solves a crisis in star formation theory termed the helium-3 problem, as shown in figure 4.

XIV. CONCLUSION AND OUTLOOK

Contrary to the current opinion, the galactic dark matter (DM) is likely of baryonic origin and observed already. It may seem ironic that nature has sequestered most of the baryonic matter in nested clumps of clumps, from planet mass to cluster and then to galactic scale. The structure predicted by the theory of gravitational hydrodynamics, micro brown dwarfs (μBDs, muBDs) grouped in Jeans clusters (JCs), is supported by an impressive body of observations: quasar microlensing, planetary nebulae, 15K cold dust temperatures, "cirrus clouds", extreme scattering events, parabolic events, direct observations and long duration radio events. This picture offers an explanation for paradoxes such as the Lyman-alpha forest, iron planet cores and young stars near the black hole in the center of the Galaxy. Globular clusters seem to arise from JCs that are heated by tidal forces when passing nearby the galaxy's central black hole. Likewise, galaxy merging turns dark JCs into young globular clusters along the merging path [15], rather than producing tidal tails of old stars that have remained unobserved [22] We summarize our findings in Table 2.

The direct search by Eros-I has concluded that the case of earth mass Machos is ruled out. However, for our μBDs the Einstein radius that describes the lensing is comparable with the physical radius of the lens object, which complicates the lensing. This motivates new MACHO searches, which we plan to start in January 2011, next "LMC season", benefiting from the improvement of CCD cameras and taking into account the finite–source and finite–lens size effects. With the JCs in front of the Magellanic clouds and the Galactic bulge to be identified first by the Planck mission, or the ones detected already as "cirrus clouds" by DIRBE, BOOMERANG and WMAP, the task is reduced to searching lensing events by μBDs in their JCs, a much more direct approach than the blind searches performed till now.

The cold dark matter paradigm seems to be left with a bleak face. In our picture its purported elementary particle has no reason to exist, because large scale structure formation can progress from gravitational hydrodynamics alone [15]. Meanwhile the expected mass budget of the Galactic dark halo is well estimated by our counting of cirrus clouds and our modeling of μBD mergings as the observed radio events. For the extra-Galactic situation, these findings are in line with the optical depth in quasar micro-lensing being of order unity. In line with this, the recent Xenon 100 cold dark matter search has ruled out all previous detection claims [3]. Massive neutrinos pose an alternative DM scenario [19], which is cosmologically sound [15]. Detection of the 1.45 eV neutrino mass in Katrin 2015 would solve the notorious dark matter riddle in a dual manner, by dark baryons for the "Oort" galactic DM, clustered according to gravitational hydrodynamics, and by massive neutrinos for the "Zwicky" cluster DM.

It would also be interesting to have more cases where the JCs can be resolved into their constituent μBDs, such as it is possible in planetary nebulae. An interesting case is the star formation region in the Galaxy in the direction Crux, where individual Jeans clusters can be identified from their 14 K thermal emission in recent images [64].

Extreme reliance on linearized theories in astrophysics seems to have seriously misguided the star formation theory. When direct simulations of gravitational perturbations in a gas cloud showed collapse, the result was dismissed as unphysical and due to numerical instability [65], and eliminated by Jeans filters. However, we consider the instability as physical, producing e.g. the discussed μBDs, and the linearized theory as oversimplified. Merging and infall of μBDs then offers a new scenario for the formation of heavier objects, from super-earths to heavy stars. This work thus motivates the numerical study of the full nonlinear hydrodynamics of structure formation and the N-body dynamics of μBD merging as a precursor to star formation and galaxy merging.

Observation	Jeans cluster	micro brown dwarf	cosmol. signif.
galaxy merging	yes	inferred	yes
quasar microlensing	inferred	yes	yes
planetary nebulae	yes	yes	yes
cold halo temperatures	–	yes	–
cirrus clouds	yes	yes	yes
extreme scattering events	inferred	yes	yes
parabolic events	–	yes	–
mysterious radio events	yes	yes	yes
direct detection T-dwarf	–	inferred	–
Ly-alpha forest	inferred	yes	inferred
Iron planet cores	–	inferred	–
BH mass – # globulars	yes	inferred	–

Table 2. Observations discussed in the text, their relation to Jeans clusters and micro brown dwarfs and their cosmological significance.

Acknowledgement. We thank James Rich for discussion of the EROS data.

[1] Oort, J. H. The force exerted by the stellar system in the direction perpendicular to the galactic plane and some related problems. *Bull. Astron. Inst. Netherl.* **6**, 249–287 (1932)
[2] Zwicky, F. Die Rotverschiebung von extragalaktischen Nebeln. *Helv. Phys. Acta* **6**, 110–127 (1933)
[3] Aprile, E. *et al.* First Dark Matter Results from the XENON100 Experiment. *arXiv:*1005.0380 (2010)
[4] Diemand, J., *et al.* Clumps and streams in the local dark matter distribution. *Nature* **454**, 735–738 (2008)
[5] Bouwens, R. J. *et al.* Constraints on the First Galaxies: $z \sim$ 10 Galaxy Candidates from HST WFC3/IR. *arXiv*:0912.4263
[6] Oesch, P. *et al.* Structure and Morphologies of z $\sim$ 7–8 Galaxies from Ultra-deep WFC3/IR Imaging of the Hubble Ultra-deep Field. *Astrophys. J.* **709**, L21–L25 (2010).
[7] Schild, R. E. & Gibson, C. H. Goodness in the Axis of Evil. *arXiv*:0802.3229 (2008)
[8] Kashlinsky, A., Atrio-Barandela, F., Kocevski, D.& Ebeling, H. A measurement of large-scale peculiar velocities of clusters of galaxies: results and cosmological implications, *Astrophys. J.* **686**, L49–L52 (2008)
[9] Elmegreen, D. M. *et al.* Galaxy Morphologies in the Hubble Ultra Deep Field: Dominance of Linear Structures at the Detection Limit. *Astrophys. J.* **631**, 85–100 (2005)
[10] Lee, J. & Komatsu, E. Bullet cluster: a challenge to ΛCDM cosmology. *Astrophys. J.* **718**, 6065 (2010)
[11] Disney, M. J. *et al.* Galaxies appear simpler than expected. *Nature* **455**, 1082–1084 (2008)
[12] Kroupa, P. *et al.* Local-Group tests of dark-matter Concordance Cosmology: Towards a new paradigm for structure formation? *arXiv*:1006.1647
[13] Gibson, C. H. Turbulence in the Ocean, Atmosphere, Galaxy, and Universe. *Appl. Mech. Rev.* **49**, 299–315 (1996)
[14] Gibson, C. H. Turbulence and turbulent mixing in natural fluids. Physica Scripta, Turbulent Mixing and beyond 2009 Proceedings, T142 (2010) *arXiv*:1005.2772.
[15] Nieuwenhuizen, T. M., Gibson, C. H. & Schild, R. E. Gravitational hydrodynamics of large-scale structure formation. *Europhys. Lett.* **88**, 49001,1–6 (2009)
[16] Geller, M. J. & Huchra, J. P. Mapping the Universe. *Science* **246**, 897–903 (1989)
[17] Rusin, D. & Kochanek, C. S. The evolution and structure of early–type field galaxies: a combined statistical analysis of gravitational lenses. *Astrophys. J.* **623**, 666–682 (2005)
[18] Hubble, E. P. Distribution of luminosity in elliptical nebulae. *Astrophys. J.* **71**, 231–276 (1930)
[19] Nieuwenhuizen, T. M. Do non-relativistic neutrinos constitute the dark matter? *Europhys. Lett.* **86**, 59001, 1–6 (2009)
[20] Gibson, C. H. & Schild, R. E. Interpretation of the Tadpole VV29 merging galaxy system using Hydro-Gravitational Theory arXiv:astro-ph/0210583 (2002)
[21] Tran, H. D., Sirianni, M. *et al.* Advanced Camera for Surveys Observations of Young Star Clusters in the Interacting Galaxy UGC 10214. *Astrophys. J.* **585** 750 (2003)
[22] Bournaud, F., Duc, P. A. & Emsellem, E., High-resolution simulations of galaxy mergers: resolving globular cluster formation. *Monthl. Not. Roy. Astron. Soc.* **389**, L8–L12 (2008)
[23] Schild, R. E. Microlensing variability of the gravitationally lensed quasar Q0957+561 A,B. *Astrophys. J.* **464**, 125–130 (1996)
[24] Pelt, J., Schild, R., Refsdal, S. & Stabell, R. Microlensing on different timescales in the lightcurves of QSO 0957+561 A,B. *Astron. & Astrophys.* **336**, 829–839 (1998)
[25] Schild, R. E. A wavelet exploration of the Q0957+561 A, B brightness record. *Astrophys. J.* **514**, 598–606 (1999).
[26] Schneider, P., Ehlers, J. & Falco, E. Gravitational Lenses. (Springer, Berlin, 1992)
[27] Schild, R. E. & Vakulik, V. Microlensing of a Ring Model for Quasar Structure. *Astron. J.* **126**, 689–695 (2003).
[28] Burud, I. *et al.* An Optical Time Delay Estimate for the Double Gravitational Lens System B1600+434. *Astrophys. J.* **544**, 117–122 (2000)
[29] Burud, I. *et al.* Time delay and lens redshift for the doubly imaged BAL quasar SBS 1520+530. *Astron. & Astrophys.* **391**, 481–486 (2002)
[30] Paraficz, D. *et al.* Microlensing variability in time-delay quasars. *Astron. & Astrophys.* **455**, L1–L4 (2006)
[31] Hora, J. L., Latter, W. B., Smith, H. A. &Marengo, M. Infrared observations of the helix planetary nebula. *Astrophys. J.* **652**, 426–441 (2006); Err. - ibid. **656**, 629 (2007).
[32] Huggins, P. J., Forveille, T., Bachiller, R., Cox, P., Ageorges, N., & Walsh, J. R. High-Resolution CO and H2 Molecular Line Imaging of a Cometary Globule in the Helix Nebula. *Astrophys. J.* **573**, L55–L58 (2002)
[33] Meaburn, J. *et al.* The nature of the cometary knots in the Helix planetary nebula (NGC 7293) *Monthl. Not. Roy. Astron. Soc.* **294**, 201– 223(1998)
[34] O'Dell, C. and Handron, K. Cometary knots in the Helix nebula. *Astron. J.* **111**, 1630–1640 (1996)
Burkert A. & O'Dell, C.R. The Structure of Cometary Knots in the Helix Nebula. *Astrophys. J.* **503**, 792–797 (1998)
[35] Meaburn, J. & Boumis, P. Flows along cometary tails in the Helix planetary nebula NGC 7293. *Monthl. Not. Roy. Astron. Soc.* **402** 381–385 (2010)
[36] Alcock, C. *et al*, The MACHO Project LMC Microlensing Results from the First Two Years and the Nature of the Galactic Dark Halo. *Astrophys. J.* **486** 697–726 (1997).
[37] Alcock, C. *et al.* The MACHO Project: Microlensing Results from 5.7 Years of LMC Observations. *Astrophys. J.* **542**,

281–307 (2000)
[38] Alcock, C. *et al.* The MACHO Project: Microlensing Detection Efficiency. *Astrophys. J. Sup.* **136**, 439–462 (2001)
[39] Aubourg, E, *et al.* Evidence for gravitational microlensing by dark objects in the Galactic halo. *Nature* **365**, 623–625 (1993)
[40] Renault, C. *et al*, Search for planetary mass objects in the Galactic halo through microlensing. *Astron. & Astrophys.* **329** 522–537 (1998)
[41] Tisserand, P. *et al.*, Limits on the Macho Content of the Galactic Halo from the EROS-2 Survey of the Magellanic Clouds. *Astron. & Astrophys.* **469**, 387–404 (2007)
[42] Udalski, A. *et al.* The optical gravitational lensing experiment. Discovery of the first candidate microlensing event in the direction of the Galactic Bulge. *Acta Astron.* **43**, 289–294 (1993)
[43] Wyrzykowski, L., *et al.* The OGLE view of microlensing towards the Magellanic Clouds I. A trickle of events in the OGLE-II LMC data. *Mon. Not. R. Astron. Soc.* **397**, 1228–1242 (2009)
[44] Sumi, T. *et al.* A Cold Neptune-Mass Planet OGLE-2007-BLG-368Lb: Cold Neptunes Are Common. *Astrophys. J.* **710**, 1641–1653 (2010)
[45] Agol, E. Occultation and microlensing. *Astrophys. J.* **579** 430–436 (2002).
[46] Lee, C. H., Seitz, S., Riffeser, A. & Bender, R. Finite-source and finite-lens effects in astrometric microlensing *arXiv*:1005.3021
[47] Marsh, K., Kirkpatrick, D. & Plavchan, P. A young planetary-mass object in the ρ Oph cloud core. *Astrophys. J.* **709**, L158–L162 (2010)
[48] Radovich, M., Kahanpaa, J. & Lemke, D. Far-infrared mapping of the starburst galaxy NGC 253 with ISOPHOT. *Astron. & Astrophys.* **377**, 73–83 (2001)
[49] Liu, G., *et al.* An Investigation of the Dust Content in the Galaxy pair NGC 1512/1510 from Near-Infrared to Millimeter Wavelengths. *Astron. J.* **139**, 1190–1198 (2010)
[50] Veneziani, M. *et al.* Properties of galactic cirrus clouds observed by BOOMERanG. *Astrophys. J.* **713**, 959–969 (2010)
[51] Walker, M. & Wardle, M. Extreme scattering events and Galactic dark matter. *Astrophys. J.* **498** L125–L128 (1998)
[52] Walker, M. Extreme scattering events: insights into interstellar medium on AU-scales. *astro-ph*/0610737.
[53] Ofek, E. O. *et al.* Long-duration radio transients lacking optical counterparts are possibly galactic neutron stars. *Astrophys. J.* **711**, 517–531 (2010).
[54] Lucas, P. Weights, D. Roche, P. & Riddick, F. Spectroscopy of planetary mass brown dwarfs in Orion. *Monthl. Not. Roy. Astron. Soc.* **373**, L60–L64 (2006)
[55] Osorio, M. R. Z., Bejar, V. J. S., Martin, E. L. *et al.* Discovery of young, isolated planetary mass objects in the sigma Orionis star cluster. *Science* **290**, 103–107 (2000).
[56] Whitworth, A. P. & Stamatellos, D. The minimum mass for star formation, and the origin of binary brown dwarfs. *Astron. & Astrophys.* **458**, 817–829 (2006)
[57] Rauch, M. The Lyman Alpha Forest in the Spectra of QSOs. *Ann. Rev. Aston. & Astrophys.* **36**, 267–316 (1998)
[58] Schild, R. E. & Dekker, M. The transparency of the Universe limited by Lyman-alpha clouds. *Aston. Nachr.* **327**, 729-732 (2006)
[59] Gibson, C. H., Schild, R. E. and Wickramasinghe, N. C., The origin of life from primordial planets, *Int. J. of Astrobiology*, (2011) doi:10.1017/S1473550410000352, *arXiv*:100.0504
[60] Lu, J.R., Ghez, A.M. *et al.* A disk of young stars at the Galactic center as determined by individual stellar orbits. *Astrophys. J.* **690**, 1463–1487 (2009)
[61] Burkert, A. & Tremaine, S. A correlation between central supermassive black holes and the globular cluster systems of early-type galaxies. *arXiv*:1004.0137.
[62] Fuller, G. M. and C. J. Smith, Nuclear weak interaction rates in primordial nucleosynthesis *Phys. Rev. D.*, 82:125017, *arXiv*:1009.0277v1 (2011)
[63] Gibson, C. H., Why the dark matter of galaxies is clumps of micro-brown-dwarfs and not Cold Dark Matter, *arXiv*:1102.1183 (2011)
[64] Photograph of star formation region in Crux: http://sci.esa.int/science-e/www/object/index.cfm?fobjectid=3D45626.
[65] Truelove, J. K. *et al.* The Jeans condition. A new constraint on spatial resolution in simulations of isothermal self-gravitational hydrodynamics. *Astrophys. J.* **489**, L179–L183 (1997)

ADDITIONAL MATERIAL

A. PROPERTIES OF JEANS CLUSTERS

Right after the transition of plasma to gas (decoupling of photons, recombination of electrons and protons) there appears fragmentation at the Jeans length, creating JCs, and inside them at the viscous length, creating μBDs [15]. Following Weinberg, we estimate the typical mass of a JC to be $6{\cdot}10^5 M_\odot$. Let M_{jc} denote the typical mass of the JCs and v_{jc} their velocity dispersion, and M_{bd} and v_{bd} the ones of the μBDs. We introduce the dimensionless variables $m_6 = M_{jc}/6 \cdot 10^5 M_\odot$, $v_{200} = v_{jc}/200$ km s^{-1}, $m_{bd} = M_{bd}/M_\oplus$, $v_{30} = v_{bd}/30$ km s^{-1}; these parameters are taken equal to unity in the main text, but kept free here and below.

For the distribution of μBDs in a JC we consider the isothermal model $\rho_{bd}(r) = v_{bd}^2/2\pi G r^2$ where $v_{bd} = v_{bd}^{rot}/\sqrt{2}$ is the velocity dispersion in terms of the rotation speed. The number density is $n_{bd} = \rho_{bd}/M_{bd}$. A JC has virial radius $R_{jc} =$

$GM_{jc}/2v_{bd}^2 = 4.4 \cdot 10^{16}(m_6/v_{30}^2)$ m and contains $N_{bd}^{jc} = 2.0 \cdot 10^{11}(m_6/m_{bd})$ μBDs. The time for a μBD to cross the JC is $R_{jc}/v_{bd} = 47,000\,(m_6/v_{30}^3)$ yr, short enough to induce the isothermal distribution because of Lynden Bell's "violent relaxation". The average mass density is $3M_{jc}/4\pi R_{jc}^3 = 3.3 \cdot 10^{-15}(v_{30}^6/m_6^2)$ kg/m^3.

Our galaxy with mass $m_{12}10^{12}M_\odot$ has a number $N_{jc} = 1.7 \cdot 10^6 m_{12}/m_6$ of JCs in its halo, that also form an ideal gas with an isothermal distribution $\rho_{jc} \equiv M_{jc}n_{jc} = v_{jc}^2/2\pi G r^2$, a shape central to the explanation of the flattening of rotation curves and the Tully-Fisher and Faber-Jackson relations [15].

B. TADPOLE GALAXY MERGING

The beginning of the wake in Fig. 1 starts at $R_{gal} = 4 \cdot 10^{21}$ m $= 420,000$ lyr from the center. Its width can be estimated at this point as $2R_{wake} = 1.5 \cdot 10^{19}$ m, and is kept fairly constant over the entire length. For spherical symmetry the mass enclosed within R_{gal} is $2v_{jc}^2 R_{gal}/G = 2.4 \cdot 10^{12} v_{200}^2 M_\odot$, a reasonable value. We estimate the number of JCs in this light path as the number in a cylinder of radius R_{wake} through the center, $N_{jc}^{wake} = \int_0^{R_{gal}} dz \int_0^{R_{wake}} \mathrm{d}r_\perp\, 2\pi r_\perp n_{jc}(\sqrt{r_\perp^2 + z^2})$, yielding the estimate $N_{jc}^{wake} = 5900\, v_{200}^2/m_6$, which is correct within a factor of a few.

C. NUMBER OF μBDs IN QUASAR MICROLENSING

Let us estimate the number of μBDs in the lens through which we observe the quasar Q0957A+B discussed in the main text. We take Hubble constant $H = 70$ km/(s Mpc). The quasar has redshift $z_Q = 1.43$ and angular distance $d_Q = 5.6 \cdot 10^{27}$ cm, the lens has $z_L = 0.355$ and $d_L = 3.2 \cdot 10^{27}$ cm. The most luminous part of the quasar is the inner ring of the accretion disk of $4 \cdot 10^{16}$ cm in diameter and 10^{14} cm wide, observed as angular diameters 1.5 μas and 3.7 nas, somewhat distorted through shear in the lens. At the position of the lens this corresponds to a luminous ring of physical diameters $d_1 = 2.3 \cdot 10^{16}$ cm and $d_2 = 5.7 \cdot 10^{13}$ cm, much less than the above JC radius, but much more than the μBD radius of $2.6 \cdot 10^{11}$ cm discussed below. The Einstein radius of an μBD in the lens is $R_E = (2/c)(GM_{bd}d_L)^{1/2} = 7.5 \cdot 10^{13} m_{bd}^{1/2}$ cm, slightly larger than d_2, so we are in the finite-source point-lens situation.

With the quasar observed in arm A under angle $\theta_A = 5''$ with respect to the center of the lensing galaxy and under $\theta_B = 1''$ in the B arm, the shortest physical distance of the light paths to the center of the lens galaxy is $r_A = \theta_A d_L = 7.8 \cdot 10^{22}$ cm and $r_B = 1.6 \cdot 10^{22}$ cm, respectively. The average number of JCs that lie along the A sight line is $N_A = n_{2D}^{jc}(r_A)\pi R_{jc}^2$, where $n_{2D}^{jc}(r) = v_{jc}^2/2GM_{jc}r$ is the projected isothermal number density. This brings $N_A = 0.002\ m_6 v_{200}^2/v_{30}^4$ and likewise $N_B = 0.01\, m_6 v_{200}^2/v_{30}^4$. Being nearly of order unity, these numbers support the fact that microlensing events are observed in both arms and put forward that each of the two sight lines of the quasar pierces through one JC.

Not having information about the distance of the sight lines to the centers of the JCs, we take for the $2D$ number density of μBDs the average value $n_{2D} = N_{bd}^{jc}/\pi R_{jc}^2$. With active area $\pi d_1 R_E$ this estimates that $18,000\, v_{30}^4/m_6\sqrt{m_{bd}}$ μBDs overlap the ring at any moment in time in either arm. The optical depth, i. e., the number of μBDs that lie inside a cylinder with radius R_E, takes the typical value $n_{2D}\,\pi R_E^2 = 58\, v_{30}^4/m_6$. (These estimates do not account for the shear). The lower values of 1.35 and 0.35 deduced from the signal analysis arise when the sight lines are near the border of the JCs, where the μBD density is lower than average. All by all, the observations are consistent with isothermal modeling of μBDs in JCs.

D. MACHOS IN FRONT OF THE MAGELLANIC CLOUDS

The Small and Large Magellanic Clouds (MCs) are satellites of the Milky Way at distance $L = 48.5$ kpc for the LMC, having $\nu\, 10^{10}$ stars in their surface of 9+84 deg^2 on the sky, with $\nu = O(1)$, per unit solid angle equivalent to $1.1\nu\, 10^8$/deg^2. The angular surface of a JC at distance xL (we take the typical JC half way, $x = \frac{1}{2}$) is $\Omega_{jc} = \pi R_{jc}^2/x^2L^2 = 3.7 \cdot 10^{-5}(m_6^2/v_{30}^4)\,\mathrm{deg}^2$, so the average number of stars of the MCs covered by a JC is $3900\,(\nu m_{jc}^2/v_{30}^4)$. The number of JCs up to distance L is $N_{jc}^L = 2v_{jc}^2 L/GM_{jc} = 1.5 \cdot 10^6(v_{200}^2/m_{jc})$, so in front of the MCs there are some 3400 v_{200}^2/m_6 JCs. They should be identified from direct thermal emission by the WMAP and Planck satellites, as foregrounds that have to be subtracted in order to study the cosmic microwave background.

When an μBD comes within the Einstein radius $R_E = \sqrt{4x(1-x)GM_{bd}L}/c = 2.6\,10^9\sqrt{m_{bd}}$ m to the sightline of a small star, it acts as a lens and enhances the intensity during a time $t_E = R_E/v_{jc} = 3.6\sqrt{m_{bd}}/v_{200}$ hrs. The μBDs that lens a given star within in a period Δt, lie in a strip on the sky with surface $\Delta O = 2R_E v_{jc}\Delta t$, which embodies $N_{bd}^{jc}\Delta O/\pi R_{jc}^2$ μBDs. This leads to a lensing event rate of $1.1\,(v_{200}v_{30}^4/\sqrt{m_{bd}}m_6)$/yr for each star covered by a JC and monitoring this frequency allows to estimate m_{jc}. With 3400 $m_6^2\nu/v_{30}^4$ stars of the MCs per JC, this leads 4100 $(m_6\nu v_{200}/\sqrt{m_{bd}})$ of Macho events per yr per JC and in total $1.4 \cdot 10^7\, \nu v_{200}^3/\sqrt{m_{bd}}$ events per year in front of the MCs.

In the Eros–I search some $2 \cdot 10^6$ stars were monitored, so we would expect some 2800 lensing events per year, while none was monitored. It was realized that the stellar radii are at least comparable to the Einstein radius (finite source); no lensing detection is made when the stellar radius exceeds 16 solar radii, which excludes a good part of the studied stars. However, also the deflector is extended (finite lens), because the Einstein radius of the μBD just coincides with our estimate for its physical

radius. This may lead to obscuration, and on top of this, there will be refraction effects from the atmosphere of the μBD: Lensing of earth mass μBDs towards the MCs appears to be a subtle case, that calls for more study.

Each JC has N_{bd}^{jc} μBDs with Einstein area $\Omega_E = \pi R_E^2/x^2L^2 = 1.2\,10^{-19} m_{bd}\,\mathrm{deg}^2$. This brings a coverage fraction or "optical depth" equal to $\tau = N_{bd}^{jc}\Omega_E N_{jc}^L/4\pi = 2v_{jc}^2/c^2 = 8.9\,10^{-7} v_{200}^2$, as is well known. But JCs themselves have a much larger optical depth, $\tau = N_{bd}^{jc}R_E^2/R_{jc}^2 = 6.7\cdot 10^{-4}(v_{30}^4/m_6)$, so it is of course advantageous to identify the JCs first and search behind them.

E. COMPOSITION OF CIRRUS CLOUDS

Fig. 3 of the cirrus clouds shows mass concentrations with kJy emission [50]. Let us assume that this DIRBE signal at $\nu = 1.25$ THz stems from thermal emission at the μBD surface with temperature 15 K, with the Planck function equal to $I_\nu = 4\pi\hbar\nu^3/[\exp(2\pi\hbar\nu/k_BT)-1]c^2 = 54$ GJy. We first investigate whether it may arise from individual μBDs. The distance to the nearest μBD can be estimated if the Sun is inside a local Jeans cluster. The typical number density $3M_{jc}/4\pi R_{jc}^3 M_{bd}$ leads to a typical distance $d_1 = 1.2\cdot 10^{15}(m_6^{2/3}m_{bd}^{1/3}/v_{30}^2)$ cm, or 82 AU, which is well before the Oort cloud, believed to start at 2000 AU. With the μBD radius taken from previous section, we get an intensity $J = I_\nu R_{bd}^2/d_1^2 = 2.4\,(t_d^2 v_{30}^6/m_6^{4/3}m_{bd}^{2/3})$ kJy, the observed scale. But the angular diameter of an μBD at this distance is 0.02°, much smaller than the structures in Fig. 3.

The signal is therefore more likely arising from JCs. Their local number density is isothermal, $n = v_{jc}^2/2\pi G M_{jc} d_{SagA^*}^2$, involving the distance 25,000 lyr to Sag. A*, and yields the typical distance to next JC as $d_2 = n^{-1/3} = 8.9\cdot 10^{18}(m_6^{1/3}/v_{200}^{2/3})$ m or 940 lyr. The $2\cdot 10^{11}$ μBDs in next JC bring together also a kJy signal, $J = N_{bd}^{jc} I_\nu R_{bd}^2/d_2^2 = 0.92\,(t_d^2 m_6^{1/3} v_{200}^{4/3} v_{30}^2/m_{bd})$ kJy. At this distance the JC diameter $2R_{jc}$ appears at an angle of $2\theta = 2R_{jc}/d_2 = (m_6^{2/3}v_{200}^{2/3}/v_{30}^2)\,0.57^\circ$, in good agreement with the largest structures of Fig. 3. The angular surface of the JC is $\Omega = \pi\theta^2$. The intensity per unit solid angle is $\mathrm{d}J/\mathrm{d}\Omega \approx J/\Omega = I_\nu N_{bd}^{jc} R_{bd}^2/\pi R_{jc}^2 \mathrm{sr} = 11.7(t_d^2 v_{30}^6/m_6 m_{bd})$ MJy/sr. Several structures in fig. 3 have the maximal intensity of 2 MJy/sr, this is achieved for JCs for proper values of t_d and m_6.

Let us estimate the number of structures in Fig. 3. Arising from JCs with equal intensity at varying distances, they form clumped structures with diameter of 1° down to, say, 0.25°, corresponding to distances $d_1 = 5.1\cdot 10^{18} m_6/v_{30}^2$ m and $d_2 = 2.0\cdot 10^{19} m_6/v_{30}^2$ m, respectively. The number of JCs in a spherical shell between them is $N_{4\pi} = 2v_{jc}^2(d_2-d_1)/GM_{bd} = 15,000 v_{200}^2/v_{30}^2$. In a DIRBE area one gets as number of JCs $N_{4\pi} 15^\circ\times 12^\circ/4\pi\mathrm{rad}^2 = 67 v_{200}^2/v_{30}^2$, which is a fair estimate for the number of structures in Fig. 3.

We can therefore conclude that these concentrations likely arise from JCs that constitute the full Galactic dark matter.

F. RATE OF μBD MERGING

We attribute the observed radio events to merging of μBDs in JCs that constitute the BDM of the Galaxy. Let us present a statistical estimate for its frequency. From the event duration t_{ev} the effective μBD radius is estimated as $R_{bd} = v_{bd}\,t_{ev} = 2.6\cdot 10^{11} t_d v_{30}$ cm. The typical JC has $N_{cell}^{jc} = (R_{jc}/R_{bd})^3$ cells of linear size R_{bd}. At a given moment in time its typical number of events, i. e., the number of μBD pairs that occupy the same cell, is of order unity, $\frac{1}{2}N_{bd}^{jc}(N_{bd}^{jc}-1)/N_{cell}^{jc} = 0.50\,t_d^3 v_{30}^9/m_6 m_{bd}^2$. The rate of mergings is this number divided by t_e, viz. $3.1\cdot 10^8(m_{12}t_d^2 v_{30}^9/m_6^2 m_{bd}^2)$/yr, corresponding to $7400\,(m_{12}t_d^2 v_{30}^9/m_6^2 m_{bd}^2)/\mathrm{deg}^2\mathrm{yr}$. This estimates fairly well the observed rate $\sim 1000/\mathrm{deg}^2\mathrm{yr}$ and the extraplolated full sky rate $4.1\,10^7$/yr is equivalent to $6\cdot 10^{17}$ merging events in the Hubble period of 14 Gyr, which amounts to two merging events per μBD. Given that all large objects, like the Sun, arise from merged μBDs, there should still be many original μBDs, and this is observed in Fig. 2 of Helix.

The amount of energy available in the merging process is large, of order GM_{bd}^2/R_{bd}, some 10^5 J/kg. Assuming this to be emitted at distance of 3 kpc during the event time of 1 day in a frequency band of 10 GHz gives a bright radio event of 1 Jy; such events are observed, see table 2 of [53].

G. LYMAN ALPHA FOREST

Let us consider a quasar of mass $M_q = m_9 10^9 M_\odot$ at redshift $z_q = 3$. It has a Schwarzschild radius $R_q = 2GM_q/c^2 = 3.0\cdot 10^{12} m_9$ m and angular distance $d_A(z_q) = 5.1\cdot 10^{25}$ m. A JC, at redshift z, is much larger, the number of its μBDs in front of the quasar $N_{bd}^q(z) = N_{bd}^{jc}(R_q/d_A(z_q))^2(d_A(z)/R_{jc})^2$ equals $890(m_9^2 v_{30}^4/m_6 m_{bd})d_A^2(z)/d_A^2(z_q)$.

JCs intersected by the quasar sight line lie in a cylinder of radius R_{jc}, so their mass can be estimated as $0.02\rho_c\cdot\pi R_{jc}^2\cdot c/H_0$, where the factors describe the average cosmic baryon density not in X-ray gas, the surface area and typical quasar distance, respectively. This corresponds to 0.0001 JCs. But the typical density in filaments between cosmic voids is $5-10$ times the average galactic density of $0.2\,M_\odot/\mathrm{pc}^3$, some $10^7\rho_c$, so the clumpedness of matter can explain that indeed μBDs cause a narrow absorption line per JC.